

## Low-lying excited states of light-harvesting system II in purple bacteria

Yang Zhao, Man-Fai Ng, and GuanHua Chen

*Department of Chemistry, University of Hong Kong, Hong Kong, People's Republic of China*

(Received 10 January 2003; revised manuscript received 25 September 2003; published 31 March 2004)

The low-lying excited states of a B850 ring of *Rhodospirillum (Rs.) molischianum* are determined accurately by a semiempirical INDO/S method. Results obtained are found to fit extremely well with a Frenkel exciton model with long-range dipolar interactions, and the spatial size of the electron-hole pair is confirmed to fall predominantly within one bacteriochlorophyll with a small leakage to its nearest neighbors. More importantly, the nearest neighbor exciton coupling constants are found to be close to those evaluated directly from dimers, and thus, an existing discrepancy between calculated results of dimers and B850 rings has been resolved.

DOI: 10.1103/PhysRevE.69.032902

PACS number(s): 87.15.-v, 87.16.Ac, 87.17.Aa

The basic energy source for virtually all organisms is photosynthesis, via which the energy of sunlight is used to convert carbon dioxide and water into the simple sugar glucose. Photosynthetic systems have developed various antenna systems in order to better capture sunlight. The structures of the light-harvesting apparatus in purple bacteria, such as *Rhodospirillum (Rs.) molischianum*, have been resolved by x-ray crystallography [1,2]. The photosynthetic unit (PSU) in these purple bacteria is composed of light-harvesting aggregates of bacteriochlorophyll (LHI and LHII), carotenoids and a reaction center (RC). The LHI (B875) aggregate encircles the reaction center while the LHII aggregate (B800 and B850) forms a peripheral network of pigment-protein complexes located next to the LHI aggregate.

The LHII complex of *Rs. molischianum* is an eight-unit circular aggregate built from  $\alpha\beta$ -heterodimers forming with  $C_8$  symmetry. Each unit contains a pair of  $\alpha$  and  $\beta$  apoproteins, three bacteriochlorophylls-a (BChls-a) molecules and one carotenoid. The BChl-a molecules form two rings named according to their corresponding absorption maxima at 800 nm and 850 nm as the B800 and B850 rings, respectively. The B850 ring consists of 16 tightly positioned BChls-a, and the B800 ring, of eight loosely spaced BChls-a, as shown in Fig. 1(a). For the B850 ring, the BChls-a binded to the  $\alpha$ -apoprotein and  $\beta$ -apoprotein are labeled as  $\alpha$ -BChl-a and  $\beta$ -BChl-a, respectively. The Mg to Mg distance is about 9.36 Å for the  $1\alpha-1\beta$  dimer, and about 8.78 Å for the  $1\beta-2\alpha$  dimer (center to center values in Ref. [3]). By eliminating the phytol tail and some alkyl groups, each BChl-a is truncated to 46 atoms [cf. Fig. 1(b)]. The total number of atoms for the B850 ring in Fig. 1(a) is thus 736. Exciton-mediated energy transfer occurs via the low-energy absorption  $Q$  band of BChl-a which includes the  $Q_y$  and  $Q_x$  transitions with transition dipole moments lying along two perpendicular directions [4,5] in the porphyrin ring as shown in Fig. 1.

Two possible mechanisms have been proposed for energy transfer dynamics from LHII to RC via LHI, namely, the Forster incoherent hopping and the coherent exciton migration. Which mechanism dominates the transfer process inside LHII is determined by dynamic and static energetic disorder in LHII as well as the dimeric coupling constants for  $1\alpha-1\beta$  and  $1\beta-2\alpha$  dimers which are denoted as  $J_1$  and  $J_2$ , respectively. Thus, central to the study of energy transfer dynamics is the evaluation of  $J_1$  and  $J_2$ . By applying the CEO method to BChl-a dimers Tretiak *et al.* [7] gave estimates of  $J_1$  and

$J_2$  to be 408 and 366  $\text{cm}^{-1}$ , respectively. Using a point-dipole approximation (PDA) Sundstrom *et al.* [3] found the  $J_1$  and  $J_2$  to be 339 and 336  $\text{cm}^{-1}$ , respectively. Cory *et al.* [8] performed an INDO/S-CIS calculation on the entire B850 ring in order to construct from the low-lying excitonic states a Frenkel exciton model with long-range dipolar interactions. Their CI expansion includes 4096 configurations for each of two symmetry representations, and their reported values for  $J_1$  and  $J_2$  are 790 and 369  $\text{cm}^{-1}$ , respectively. From *ab initio* molecular orbital calculations Scholes *et al.* [6] estimated the couplings  $J_1$  and  $J_2$  in the B850 ring of *Rps. acidophila* to be 320 and 255  $\text{cm}^{-1}$ , respectively. With the exception of work done by Schulten, Zerner and co-workers on entire B850 rings [8], all other calculations were on absorption spectra of monomers or dimers. Calculated values for  $J_1$  and  $J_2$  vary from 300  $\text{cm}^{-1}$  to 800  $\text{cm}^{-1}$  while calculated results from dimers differ significantly from those of the entire rings. One possible cause for the discrepancy is that long range Coulombic interactions are absent in the calculation of dimers. The long range interactions may affect the exciton wavefunctions significantly. A drawback of the INDO/S-CIS calculations is the cutoff of molecular orbitals near the highest occupied and lowest unoccupied molecular orbitals, which may lead to an overestimation of  $J_1$  and  $J_2$ . Here we employ an accurate linear-scaling localized-density-matrix (LDM) at the INDO/S level to calculate the low-lying excited state energies of the B850 ring. Developed for computing the excited state properties of large molecular systems, the LDM method has been previously employed to calculate the absorption spectra of polyacetylene oligomers [9] and carbon nanotubes [10].

The INDO/S Hamiltonian in the presence of an external field  $\mathbf{E}$  reads [11]

$$\begin{aligned}
 H = & \sum_{ab} \sum_{i \in a, j \in b} t_{ij} c_{ai}^\dagger c_{bj} + \frac{1}{2} \sum_a \sum_{ijmn} V_a^{ij, mn} c_{ai}^\dagger c_{am}^\dagger c_{an} c_{aj} \\
 & + \frac{1}{2} \sum_{a \neq b} \sum_{i \in a, j \in b} \gamma_{ab}^{ij} c_{ai}^\dagger c_{ai} c_{bj}^\dagger c_{bj} - \mathbf{E} \cdot \sum_{mn} \mathbf{P}_{ab}^{mn} c_{am}^\dagger c_{bn},
 \end{aligned} \tag{1}$$

where  $c_{ai}^\dagger$  ( $c_{bj}$ ) is the creation (annihilation) operator for an electron at a localized atomic spin spatial orbital  $i$  ( $j$ ) on atom  $a$  ( $b$ ).  $t_{ij}$  is the one-electron hopping term,  $V_a^{ij, mn}$  is one-center repulsion term and  $\gamma_{ab}^{ij}$  is the two-center repulsion

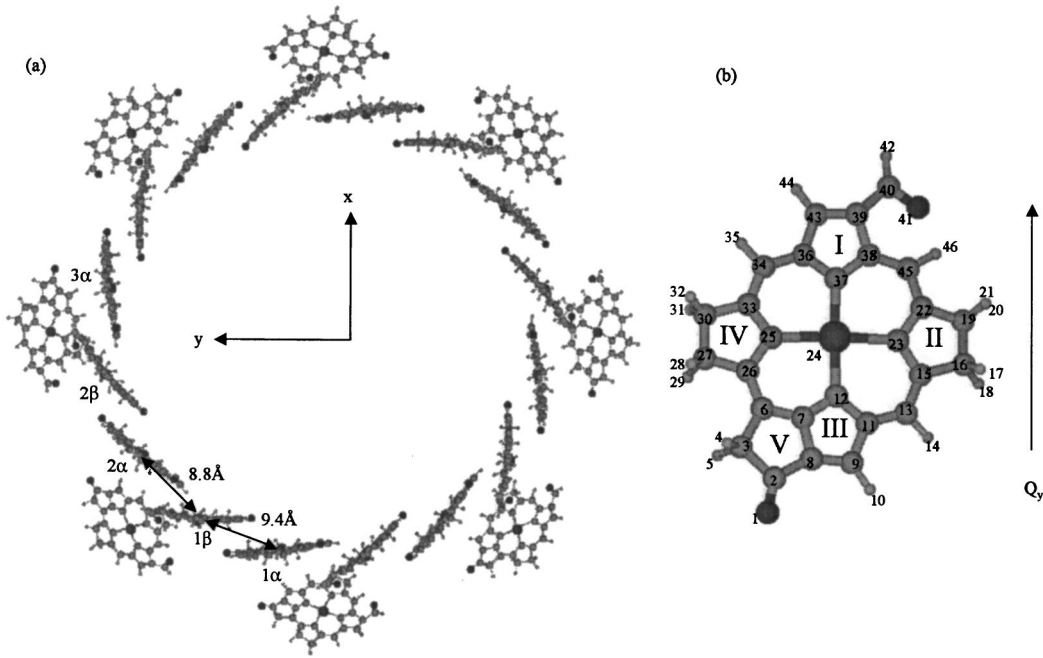


FIG. 1. (a) The entire LHII with labeling scheme. Note that the Mg to Mg distances for the  $1\alpha$ - $1\beta$  dimer,  $1\beta$ - $2\alpha$  dimer,  $1\alpha$ - $2\alpha$  dimer,  $1\beta$ - $2\beta$  dimer,  $1\alpha$ - $2\beta$  dimer and  $1\beta$ - $3\alpha$  dimer are 9.4, 8.8, 17.4, 18.0, 26.0, and 25.5 Å, respectively. The outer ring is the B800 ring while the inner ring is B850 ring. (b) The truncated bacteriochlorophyll-a (BChl-a) which contains 46 atoms and with the atom index.

term. The second and the third terms in Eq. (1) represent the effective electron-electron Coulomb interaction. The last term labels the interaction between the valence electrons and an external electric field  $\mathbf{E}(t)$ , and  $\hat{\mathbf{P}}$  is the molecular dipole moment operator.  $\mathbf{P}_{ab}^{ij}$  is calculated by  $\langle \chi_a^i | \hat{\mathbf{P}} | \chi_b^j \rangle$ , where  $\chi_a^i$  ( $\chi_b^j$ ) stands for the  $i$ th ( $j$ th) atomic orbital of atom  $a$  ( $b$ ), neglecting the diatomic overlap. The INDO/S parameters used in these calculations are from Ref. [12] by Zerner *et al.* The geometry is based on the recently resolved crystal structure of the *Rs. molischianum* complex [2], obtained from the Protein Data Bank of the Research Collaboratory for Structural Bioinformatics. Hydrogen atoms are added using the InsightII software.

The  $Q_y$  ( $Q_x$ ) transition energies for  $\alpha$ -BChl-a and  $\beta$ -BChl-a are 1.17 eV (2.16 eV) and 1.15 eV (1.98 eV), respectively. The  $Q_y$  transition carries the strongest oscillator strength. In contrast to a symmetric porphyrin molecule, the asymmetric BChl-a molecule has a significant dipole strength for the  $Q_y$  transition [13]. The  $Q_x$  transition is weakly dipole allowed. Proteins in LHII are generally believed to provide only structural support, and therefore, do not significantly affect the electronic structures. Carotenoids absorb light at about 2.5 eV, and are expected not to intervene in the low-lying excitations. Our calculations confirm that the  $Q_y$  transition is red-shifted little with an added protein environment and carotenoids ( $<0.01$  eV). Therefore, the proteins and carotenoids are removed in subsequent calculations.

The absorption energies for  $Q_{y1}$  and  $Q_{y2}$  for the  $1\alpha$ - $1\beta$  ( $1\beta$ - $2\alpha$ ) dimer are 1.08 eV and 1.21 eV (1.09 eV and 1.21 eV), respectively. It follows that the electronic splitting for the  $1\alpha$ - $1\beta$  ( $1\beta$ - $2\alpha$ ) dimer are 0.132 eV (0.114 eV). These values are somewhat larger than those from Ref. [7] (0.102

eV and 0.091 eV for the  $1\alpha$ - $1\beta$  dimer and the  $1\beta$ - $2\alpha$  dimer, respectively). One reason for the discrepancy is that slightly different geometries are used in the two calculations. Adopting a procedure employed in Ref. [7], we arrive at an estimation of inter-monomer coupling constants for two types of dimers,  $J_1 = 528 \text{ cm}^{-1}$  for the  $1\alpha$ - $1\beta$  dimer and  $J_2 = 455 \text{ cm}^{-1}$  for the  $1\beta$ - $2\alpha$  dimer, which are compared with coupling constants obtained via other methods in Table I.

To determine an appropriate density-matrix cutoff length for the B850 ring, we carried out calculations on trimers and pentamers with and without the density-matrix truncations. The off-diagonal elements of reduced single-electron density matrix between nearest BChl-a neighbors are fully included if the density matrix is truncated by a cutoff length of 15 Å. Absorption spectra obtained from calculations with and without the 15-Å cutoff are found to be nearly identical. For instance, the pentamer lowest absorption peaks are found at 0.99 eV for spectra calculated both with and without the 15-Å cutoff. The fact that the absorption spectra of trimers and pentamers differ little upon the introduction of the cutoff length 15 Å confirms that the spatial extent (or the electron-hole distance) of low-lying excitons is confined to two BChls-a. Further analysis of the resulting density matrices of

TABLE I. Calculated coupling constants for the two types of dimers:  $J_1$  for the  $1\alpha$ - $1\beta$  dimer, and  $J_2$  for the  $1\beta$ - $2\alpha$  dimer. Our LDM results are compared with those from the CEO approach [7], the ZINDO method [8], and the PDA approximation [3].

Method	LDM	LDM	CEO	ZINDO	PDA
Configuration	dimer	ring	dimer	ring	dimer
$J_1$ ( $1\alpha$ - $1\beta$ , $\text{cm}^{-1}$ )	528	593	408	790	339
$J_2$ ( $1\beta$ - $2\alpha$ , $\text{cm}^{-1}$ )	455	491	366	369	336

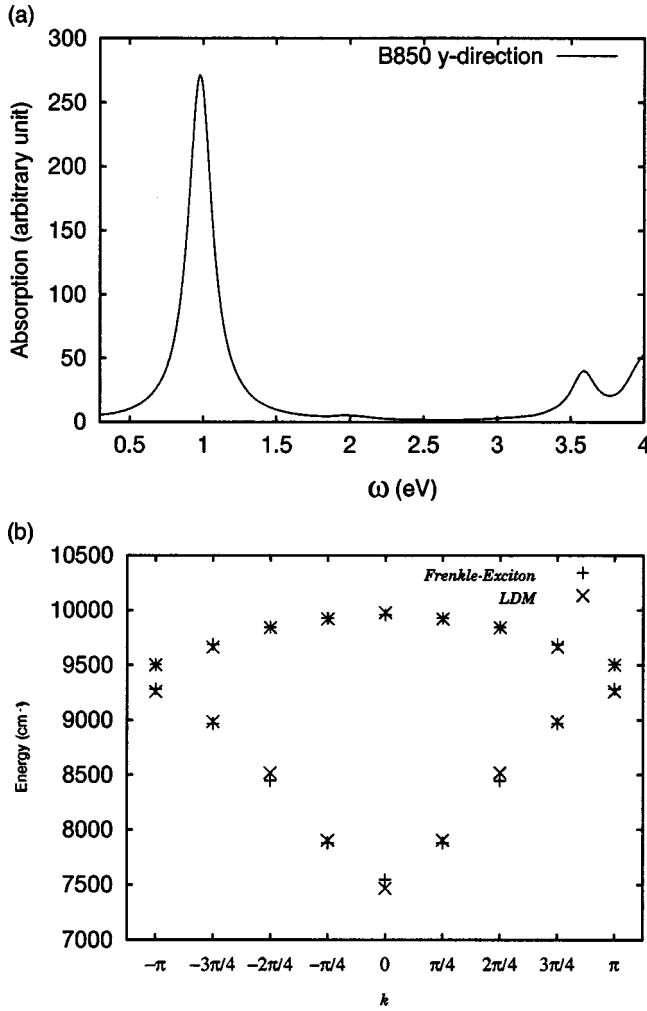


FIG. 2. (a) Absorption spectrum for an entire B850 ring with a cutoff length of 15 Å. (b) Ten energy levels extracted from the absorption spectra or fictitious spectra (cross), and ten corresponding fitted eigenvalues from a dimerized Hamiltonian with additional dipolar interactions between non-nearest BChl-a neighbors (plus). The fitting parameters are  $J_1=594 \text{ cm}^{-1}$ ,  $J_2=491 \text{ cm}^{-1}$ ,  $\epsilon_1=\epsilon_2=9117 \text{ cm}^{-1}$ , and  $C=640725 \text{ \AA}^3 \text{ cm}^{-1}$ . The  $x$  axis is labeled by the crystal momenta of the exciton  $p = \pm K\pi/4$  ( $K=0,1,2,3,4$ ).

the excitons finds that the size of the electron-hole pair is mostly limited to one BChl-a.

Dimerization splits the one-exciton band of the B850 ring into a lower band and an upper band. The only significant dipole-allowed excitation occur between the ground state and the excited states with momenta  $k = \pm \pi/4$  of the lower one-exciton band along the ring [14]. Figure 2(a) shows the absorption spectrum of a B850 ring with a cutoff length of 15 Å. The major absorption peak at low energies is attributed to the  $k = \pm \pi/4$  state in the lower exciton band. The other 14 low-lying excited states have little or no oscillator strengths, and therefore, can not be resolved from Fig. 2(a). Instead of resorting to nonlinear spectroscopy, we introduce fictitious external fields with an individual phase on each BChl-a in the B850 ring. One may flip the orientation of (i.e., adding a  $180^\circ$  phase to) the external field on the eight monomers in the upper half of the ring so that dipole-allowed transitions

TABLE II. Spectrum of the entire B850 ring calculated by the INDO/S-LDM method in the gas phase, from which we have obtained via a fitting procedure:  $J_1=594 \text{ cm}^{-1}$ ,  $J_2=491 \text{ cm}^{-1}$ ,  $\epsilon_1=\epsilon_2=9117 \text{ cm}^{-1}$ , and  $C=640725 \text{ \AA}^3 \text{ cm}^{-1}$ .

	Lower band ( $\text{cm}^{-1}$ )	Upper band ( $\text{cm}^{-1}$ )
$k=0$	7469	9501
$k=\pm \pi/4$	7904	9663
$k=\pm \pi/2$	8517	9840
$k=\pm 3\pi/4$	8985	9921
$k=\pi$	9259	9977

are now from the ground state to one-exciton excited states of momenta  $k=0, \pm \pi/2, \pi$  of the lower band, and  $k = \pm \pi/2, \pi$  of the upper band. The previous allowed  $k = \pm \pi/4$  states of the lower band, however, are no longer optically bright. Similar techniques can be applied to find out other symmetry forbidden transitions. For example, one may flip the orientation of the external field on even-numbered monomers in the B850 ring to obtain optical transitions to  $k = \pm 3\pi/4$  state of the upper band. The complete spectrum of the B850 ring was thus resolved, and results are displayed in Table II.

We find that a simple excitonic model for a dimerized LHII ring incorporating only nearest-neighbor interactions can not fit our calculated results. Schulten and co-workers have introduced a more realistic description of the hexadecamer that takes the form of the Hamiltonian

$$\hat{H} = \begin{pmatrix} \epsilon_1 & J_1 & W_{1,3} & \cdot & \cdot & \cdot & J_2 \\ J_1 & \epsilon_2 & J_2 & \cdot & \cdot & \cdot & W_{2,2N} \\ W_{3,1} & J_2 & \epsilon_1 & \cdot & \cdot & \cdot & \cdot \\ \cdot & \cdot & \cdot & \cdot & \cdot & \cdot & \cdot \\ \cdot & \cdot & \cdot & \cdot & \epsilon_2 & J_2 & W_{2N-2,2N} \\ \cdot & \cdot & \cdot & \cdot & J_2 & \epsilon_1 & J_1 \\ J_2 & \cdot & \cdot & \cdot & W_{2N,2N-2} & J_1 & \epsilon_2 \end{pmatrix} \quad (2)$$

where  $\epsilon_1$  and  $\epsilon_2$  are the excitation energies of the  $Q_y$  state of an individual BChl-a,  $J_1$  and  $J_2$  are the coupling constants between the nearest neighbors, and  $N$  equals 8 as the system is of  $C_8$  symmetry. In addition to the nearest-neighbor interactions  $J_1$  and  $J_2$ , the matrix  $W_{i,j}$  in Eq. (2) adds dipolar couplings due to non-nearest neighbors:

$$W_{i,j} = C \left[ \frac{\mathbf{d}_i \cdot \mathbf{d}_j}{|\mathbf{r}_{ij}|^3} - \frac{(\mathbf{d}_i \cdot \mathbf{r}_{ij})(\mathbf{d}_j \cdot \mathbf{r}_{ij})}{|\mathbf{r}_{ij}|^5} \right], \quad (3)$$

where the factor  $C$  is the proportionality constant to be determined, and  $\mathbf{r}_{ij}$  is the vector connecting the  $i$ th and  $j$ th monomers. The direction of the transition dipole of the  $i$ th BChl-a is represented by a unit vector  $\mathbf{d}_i$ .

A least-square fit to the low-lying excited state energies is utilized to determine  $J_1$ ,  $J_2$ ,  $\epsilon_1$ ,  $\epsilon_2$  and  $C$  in Eq. (2). To ensure that the sum of the low-lying excited state energies is invariant, a constraint is imposed during the fitting procedure:

$$8\epsilon_1 + 8\epsilon_2 = \sum_k E_k, \quad (4)$$

where  $E_k$  is the energy of the eigenstate  $k$ . The agreement between the LDM results and the Frenkel exciton model is excellent. In Fig. 2(b), the INDO/S-LDM result is represented by crosses, and the fitting result by pluses. The total rms error is  $118 \text{ cm}^{-1}$ . The corresponding parameters are  $J_1 = 594 \text{ cm}^{-1}$ ,  $J_2 = 491 \text{ cm}^{-1}$ ,  $\epsilon_1 = \epsilon_2 = 9117 \text{ cm}^{-1}$ , and  $C = 640725 \text{ \AA}^3 \text{ cm}^{-1}$ . Compared with the results in Ref. [8] our results are much more in line with those calculated directly from the dimer results. To further justify the parametrized Frenkel exciton Hamiltonian, we calculate the transition dipole moment  $\mu$  of the monomer  $Q_y$  state and obtain  $\mu = 2.326e \cdot \text{\AA}$ . Assuming each BChl-a in the B850 ring has the same transition dipole as that of a monomer, and the coupling among the transition dipoles are described by Eq. (3),  $C$  is found to be  $639800 \text{ \AA}^3 \text{ cm}^{-1}$ , which is consistent with the fitting result for the entire B850 ring ( $640725 \text{ \AA}^3 \text{ cm}^{-1}$ ).

Transition dipoles of the chromophores approximately form a head-to-tail pattern with neighboring dipoles oriented in opposite directions. The ensuing polarization effect on the BChls-a is partially responsible for the vanishing  $\epsilon_1 - \epsilon_2$  for a B850 ring. Compared with a center BChl-a in a trimer, a BChl-a in a ring experiences an additional long-range dipolar field from 13 other BChls-a. Energies due to the ground-state dipolar fields acting on a specific  $\alpha$ -BChl-a or a  $\beta$ -BChl-a due to its non-nearest neighbors are found to be  $-194$  and  $-153 \text{ cm}^{-1}$ , respectively. Due to differing long-range dipolar fields on adjacent BChls-a, the difference between  $\epsilon_1$  and  $\epsilon_2$  is found to be significantly reduced.

So far our molecules are treated in the gas phase. To take into account solvent effects, the ground state Fock operator is modified by adding the Onsager dipolar term [15,16]. Solvent effects are found to increase the ground state dipole moment from 7.7 to 22.0 D, in agreement with other studies [7,8]. For the excited state, the Hamiltonian term due to interactions with the external fields is modified to [16]

$$\hat{H}_{ext} = -\mathbf{E} \cdot (\widehat{\mu}_g + \widehat{\delta\mu}) - \left[ \frac{D' - 1}{2D' + 1} + \frac{2(\eta^2 - 1)}{2\eta^2 + 1} \right] \widehat{\mu}_g \cdot \widehat{\delta\mu}, \quad (5)$$

where  $\widehat{\mu}_g$  and  $\widehat{\delta\mu}$  are the ground-state and field-induced dipole moments, respectively,  $\eta$  is the index of refraction due to instantaneous response of the solvent electrons ( $\eta \approx 1.6$  [17]), and  $D'$  is the contribution to the bulk dielectric due to orientations of the solvent molecules ( $D' = 1.75$ ). The  $Q_y$  peak of  $\alpha$ -BChl-a is shifted from 1.17 to 1.42 eV while the  $Q_x$  peak remains at about 2.15 eV (experimentally, the peaks are found at 1.60 and 2.16 eV for the  $Q_y$  and  $Q_x$  excitations, respectively [18]). Applying Eq. (5) to dimers, we find that both  $J_1$  and  $J_2$  are reduced by 25%. Therefore, we estimate that the solvent-adjusted coupling constants  $J_1$  and  $J_2$  of a B850 ring are 445 and 368  $\text{cm}^{-1}$ , respectively, which are consistent with experimental findings [19].

We have successfully carried out a sophisticated electronic structure calculation for a B800 ring with 16 BChls-a in *Rs. molischanum*. All valence electrons are included explicitly for 736 atoms and 2176 orbitals in the B850 ring. Our calculations were done with relatively inexpensive computational resources (700-MHz CPU and 500-MB memory). Therefore, this work has demonstrated that the INDO/S-LDM approach is well-suited for very-large-scale electronic structure calculations. Our calculation shows clearly that the electron-hole pair is predominantly localized on one BChl-a with a tiny charge-transfer component between two neighboring BChls-a, and thus the excitons are of the Frenkel type. The calculated low-lying excited state energies are fitted extremely well with the Frenkel exciton Hamiltonian with long-range dipolar interactions. In addition, the so-obtained parameters of the dipolar Frenkel exciton Hamiltonian can be well accounted for by the calculated results of the monomers and dimers, and the  $J_1$  and  $J_2$  values of the B850 ring are consistent with those of the dimers. All these show that the Frenkel exciton model provides an accurate description of the low-lying excited states in the B850 ring.

Support from the Hong Kong Research Grant Council (RGC) and the Committee for Research and Conference Grants (CRCG) of the University of Hong Kong is gratefully acknowledged. The authors thank S. Yokojima and W. Z. Liang for making the LDM codes available for the calculations.

- 
- [1] G. McDermott *et al.*, Nature (London) **374**, 517 (1995).  
 [2] J. Koepke *et al.*, Structure **4**, 581 (1996).  
 [3] V. Sundström *et al.*, J. Phys. Chem. B **103**, 2327 (1999).  
 [4] M. Gouterman, J. Mol. Spectrosc. **6**, 138 (1961).  
 [5] C. Weiss, J. Mol. Spectrosc. **44**, 37 (1972).  
 [6] G.D. Scholes *et al.*, J. Phys. Chem. B **103**, 2543 (1999).  
 [7] S. Tretiak *et al.*, J. Phys. Chem. B **104**, 4519 (2000); **104**, 9540 (2000).  
 [8] M.G. Cory *et al.*, J. Phys. Chem. B **102**, 7640 (1998); X. Hu *et al.*, *ibid.* **101**, 3854 (1997).  
 [9] S. Yokojima *et al.*, Chem. Phys. Lett. **292**, 379 (1998); Phys. Rev. B **59**, 7259 (1999); W.Z. Liang *et al.*, J. Phys. Chem. A **104**, 2445 (2000).  
 [10] W.Z. Liang *et al.*, J. Am. Chem. Soc. **122**, 11129 (2000); **123**, 9830 (2001).  
 [11] J. Ridley *et al.*, Theor. Chim. Acta **32**, 111 (1973).  
 [12] A.D. Bacon *et al.*, Theor. Chim. Acta **53**, 21 (1979).  
 [13] S. Tretiak *et al.*, Chem. Phys. Lett. **297**, 357 (1998).  
 [14] T. Meier *et al.*, J. Chem. Phys. **107**, 3876 (1997).  
 [15] G. Karlsson *et al.*, Int. J. Quantum Chem. **7**, 35 (1973).  
 [16] M.M. Karelson *et al.*, J. Phys. Chem. **96**, 6949 (1992).  
 [17] F.J. Kleima *et al.*, Biophys. J. **78**, 344 (2000).  
 [18] Oelze, J. Methods Microbiol. **18**, 257 (1985).  
 [19] R. Kumble *et al.*, Chem. Phys. Lett. **261**, 396 (1996); D.C. Arnett *et al.*, J. Phys. Chem. B **103**, 2014 (1999).